

# Free convection in geophysical processes

V. V. Alekseev and A. M. Gusev

*M. V. Lomonosov Moscow State University*  
Usp. Fiz. Nauk **141**, 311–342 (October 1983)

A highly significant geophysical process, free convection, is examined. Thermal convection often controls the dynamical behavior in several of the earth's envelopes: the atmosphere, ocean, and mantle. Section 2 sets forth the thermohydrodynamic equations that describe convection in a compressible or incompressible fluid, thermochemical convection, and convection in the presence of thermal diffusion. Section 3 reviews the mechanisms for the origin of the global atmospheric and oceanic circulation. Interlatitudinal convection and jet streams are discussed, as well as monsoon circulation and the mean meridional circulation of ocean waters due to the temperature and salinity gradients. Also described are the hypotheses for convective motion in the mantle and the thermal-wave (moving flame) mechanism for inducing global circulation (the atmospheres of Venus and Mars provide illustrations). Eddy formation by convection in a centrifugal force field is considered. Section 4 deals with medium- and small-scale convective processes, including hurricane systems with phase transitions, cellular cloud structure, and convection penetrating into the ocean, with its stepped vertical temperature and salinity microstructure. Self-oscillatory processes involving convection in fresh-water basins are discussed, including effects due to the anomalous ( $\rho, T$ ) relation for water.

PACS numbers: 92.60.Ek, 94.10.Lf, 92.10. — c, 91.35.Dc

## CONTENTS

1. Introduction . . . . .	906
2. The equations of convection . . . . .	907
3. Large-scale convective motions . . . . .	908
a. Interlatitudinal air circulation and jet streams. b. Monsoon circulation. c. Mean meridional circulation in the World Ocean. d. Mantle convection. e. Atmospheric convection induced by motion of terminator. f. Convection in centrifugal force field	
4. Medium- and small-scale convection . . . . .	916
5. Closing remarks . . . . .	920
References . . . . .	920

## 1. INTRODUCTION

Free convection is a very intricate process, one that by no means has been fully explored. Highly complicated effects occur in the earth's atmosphere, hydrosphere, mantle, and core because of their great size, the diurnal rotation, and the complex thermal and density fields that exist in the outer envelopes and interior regions of our planet.

Nearly all the motions in the atmosphere ultimately owe their origin to free convection. In the ocean, some (80–90)% of the energy of motion stems from the convective movements of the atmosphere; the remaining (10–20)% reflects free convection that develops in the ocean itself. Moreover, it is not almost beyond dispute that for a long time the earth's mantle has been flowing, taking part in the convective motions; and convection may be at work in the planet's core as well.

There are two main types of free convection: Rayleigh convection, resulting from a superadiabatic vertical density gradient, the thermal and density parameters being uniform horizontally, and lateral convection, which occurs if these parameters are nonuniform.

Examples of lateral convection in the terrestrial atmosphere include the interlatitudinal air circulation due to the nonuniform thermal conditions at different latitudes, the monsoon-type circulation associated with permanent or seasonal disparities in the thermal regime above the continents and oceans, and the breeze circulation that arises from the unequal heating of sea

and land surfaces or of different land areas as their thermal environment fluctuates diurnally.

As for the classical vertical Rayleigh convection in the atmosphere, a good example is the convection that causes small clouds in a honeycomb configuration to form above large open spaces. The convection responsible for thunderclouds is of the same type. Of special significance is the vertical convection found in tropical hurricanes: it results from the vertical temperature gradient due to phase transitions between vapor and water. The oceanic analog to the interlatitudinal atmospheric convection is the mean meridional circulation induced by the lateral convection which occurs through sinkage of surface waters in certain polar seas. Lateral convection comparable in scale to the monsoon convection is not typical of the World Ocean; in general it can develop only in Antarctic waters.

Abundant instances can be cited of medium-scale lateral convection in the World Ocean. Such processes are encountered in straits joining seas whose waters differ in temperature and salinity, and in the convergence of temperature and salinity that is particularly often observed near shores where water is being freshened by drainage.

Vertical oceanic convection for the most part results from the cooling of surface waters that have become salinated through evaporation, with accompanying submergence. The process is induced by the diurnal air-temperature variation at the water surface, by sporadic changes in air temperature, by the chilling in autumn

and winter, and finally, by the continual chill in the polar regions. Accordingly the convection embraces ever deeper layers of the ocean. Local, small-scale horizontal irregularities in the cooling tend to generate fine-scale local lateral convections which give rise to *thermohaline* (or thermosolutal) vertical fine structure, the waters becoming stratified in salt content within the seasonal thermocline (steep-gradient layer).

While rising convection is on the whole more typical of the atmosphere, sinking convection, as we shall see, is characteristic of the ocean.

In the terrestrial mantle, vertical convection has produced and may still be producing differentiation of the material in the earth; iron, for example, may melt out and sink into the core. Some investigators believe that convection in the mantle is responsible for buildup of the ocean floor, for creating the deep-water troughs, and indeed for lithospheric plate tectonics generally.

Geophysical processes, of course, hold no monopoly on convection. On the one hand, convection is very often encountered in engineering practice; on the other, it occurs in the atmospheres of other planets, on the sun, in stellar interiors. But despite the enormous range in the viscosity, thermal conductivity, and other parameters of the various media in which convection develops, it possesses enough general properties for the different cases to be treated from a unified point of view.

A great deal of research has been done on convection, and a very long article would be needed to give even a cursory description. Therefore we will not attempt to consider the aspects of convection met with in applied problems, or convection on other planets (except in Sec. 3e), the sun, and stars. The convection in the earth's interior will be touched on briefly (Sec. 3d). We shall concentrate on the convective phenomena in the ocean and atmosphere of our planet: they have immense significance for an understanding of the whole process of thermal and dynamical interaction. But even here we are compelled for lack of space to limit ourselves to the principal, most typical instances of convection. Nor do we claim to give an exhaustive bibliography of the subject, although we do mention all the most important studies.

Our survey will begin with a theoretical description of convective processes and the pertinent mathematical model. Then we consider in turn the hierarchy of examples of geophysical convection set forth above, and the physics of the underlying phenomena.

## 2. THE EQUATIONS OF CONVECTION

a. The convective motion of a fluid is described (see standard texts<sup>1</sup>) by the Navier-Stokes and heat equations together with the equations of continuity and state:

$$\left. \begin{aligned} \frac{\partial \mathbf{v}}{\partial t} + (\mathbf{v}\nabla)\mathbf{v} &= \frac{1}{\rho} \nabla P + \nu \Delta \mathbf{v} + \mathbf{g}, \\ \frac{\partial T}{\partial t} + (\mathbf{v}\nabla)T &= \kappa \Delta T + \Phi, \\ \frac{\partial \rho}{\partial t} + \operatorname{div}(\rho \mathbf{v}) &= 0, \\ \rho &= \rho(T, P), \end{aligned} \right\} \quad (1)$$

where  $\mathbf{v}$  is the velocity vector;  $P$ ,  $\rho$ ,  $T$  denote pressure, density, and temperature;  $\kappa$  is the thermal conductivity coefficient,  $\nu$  is the kinematic viscosity,  $\mathbf{g}$  denotes the free-fall acceleration, and  $\Phi$  is a dissipation function.

The problems encountered in geophysical convection may be divided into two classes. In problems of the first kind, those typical of the oceans and the mantle, the pressure dependence of the density may be considered weak compared with its temperature dependence (the Boussinesq approximation). The second class of problems, to which the Boussinesq approximation is inapplicable, require that the equations of deep convection be solved. Problems of this kind occur in studies of atmospheric circulation. In geophysical contexts one may usually neglect the dissipation of energy into heat through internal friction, as well as the temperature dependence of the viscosity and thermal conductivity; the system (1) then becomes much simpler.

Let us express the temperature, pressure, and density in the form

$$T = T_0 + T', \quad P = P_0 + P', \quad \rho = \rho_0 + \rho',$$

where  $P_0 = \rho_0 \mathbf{g} \mathbf{x}$ ,  $\rho_0$ ,  $T_0$  are constant mean values, while  $T'$ ,  $\rho'$ ,  $P'$  represent small increments. Then the term  $\rho^{-1} \nabla P$  on the right in the Navier-Stokes relation may be rewritten as

$$\begin{aligned} \frac{1}{\rho} \nabla P &= \frac{1}{\rho_0 + \rho'} \nabla(P_0 + P') = \frac{1}{\rho_0} \left[ \frac{1}{1 + (\rho'/\rho_0)} \right] \nabla(P_0 + P') \\ &= \frac{1}{\rho_0} \nabla P_0 - \frac{\rho'}{\rho_0^2} \nabla P_0 + \frac{1}{\rho_0} \nabla P' - \frac{\rho'}{\rho_0^2} \nabla P' + \dots, \end{aligned}$$

so that to second-order terms in  $\rho'$ ,  $P'$  the Navier-Stokes equation will transform to

$$\frac{\partial \mathbf{v}}{\partial t} + (\mathbf{v}\nabla)\mathbf{v} = -\frac{1}{\rho_0} \nabla P' + \nu \Delta \mathbf{v} - \mathbf{g} \frac{\rho'}{\rho_0}$$

(the  $\nu$  axis points vertically upward).

Neglecting the dissipation term  $\Phi$  in the heat equation, we arrive at the following system of equations for thermal convection in the Boussinesq approximation:

$$\left. \begin{aligned} \frac{\partial \mathbf{v}}{\partial t} + (\mathbf{v}\nabla)\mathbf{v} &= -\frac{1}{\rho_0} \nabla P' + \nu \Delta \mathbf{v} - \mathbf{g} \frac{\rho'}{\rho_0}, \\ \frac{\partial T'}{\partial t} + (\mathbf{v}\nabla)T' &= \kappa \Delta T', \\ \operatorname{div} \mathbf{v} &= 0. \end{aligned} \right\} \quad (2)$$

We here assume a standard fluid whose density falls off monotonically with rising temperature:

$$\rho(T) = \rho_0(T_0)(1 - \beta T'), \quad (3)$$

where  $\beta$  is the volume expansion coefficient of the fluid.

It is a familiar fact that in fresh-water basins the density depends anomalously on temperature at values close to 4°C: the water density increases as  $T$  rises from 0°C to 4°C, reaches a maximum at about 4°C, and then diminishes again. Throughout the range from 0°C to about 30°C the equation of state for fresh water may be approximated by

$$\rho(T) = \rho_0(4^\circ\text{C}) [1 - \gamma_1(T - 4^\circ\text{C})^2 - \gamma_2(T - 4^\circ\text{C})^3], \quad (4)$$

where  $\gamma_1$ ,  $\gamma_2$  are constants.

b. Sea water is a salt solution. Evaporation in the top

layer enhances the salt concentration there and can induce convective motion. When the changing salt concentration  $S$  is included, the Navier–Stokes relation acquires an additional Archimedean term:

$$\frac{\partial \mathbf{v}}{\partial t} + (\mathbf{v}\nabla)\mathbf{v} = \frac{1}{\rho}\nabla P + \gamma\Delta\mathbf{v} + \mathbf{g}(\beta_1 T - \beta_2 S). \quad (5)$$

In this event the system (1) has to be supplemented by an equation for the salt concentration:

$$\frac{\partial S}{\partial t} + (\mathbf{v}\nabla)S = D_s\Delta S; \quad (6)$$

here  $D_s$  is the salt diffusion coefficient. Equation (6) neglects thermal diffusion; if it is significant, the salt-concentration and heat equations will take the form<sup>1</sup>

$$\begin{aligned} \frac{\partial S}{\partial t} + (\mathbf{v}\nabla)S &= D\Delta S + \alpha D_s\Delta T, \\ \frac{\partial T}{\partial t} + (\mathbf{v}\nabla)T &= (x + \alpha^2 D_s N)\Delta T + \alpha D_s N\Delta S, \end{aligned} \quad (7)$$

where  $\alpha = k_t/T$ , with  $k_t$  the thermal diffusivity; the quantity

$$N = \left[ \frac{T}{C_p} \left( \frac{\partial \mu}{\partial S} \right)_{T, P} \right]_0,$$

where  $C_p$  is the specific heat at constant pressure and  $\mu$  is the effective chemical potential.

c. The quantity  $H = C_p/\alpha g$  may be interpreted as the characteristic thickness of the layer stratified by the gravity field. As Hewitt *et al.* have shown,<sup>2</sup> the Boussinesq approximation is valid only for much shallower layers. In air,  $H = 32$  km; for water<sup>3</sup> at 20°C,  $H \approx 2000$  km; and for the upper mantle,  $H \approx 6000$  km. According to McKenzie the quantities

$$\alpha = 2 \cdot 10^{-5} \text{ } ^\circ\text{K}^{-1}, \quad C_p = 1,2 \cdot 10^3 \text{ J} \cdot \text{kg}^{-1} \cdot \text{ } ^\circ\text{K}^{-1}$$

Thus in the atmosphere the Boussinesq approximation can be used only for convection in quite thin layers of air; it would be wrong to apply it to the whole atmosphere.

Consequently the “deep convection” equations<sup>4</sup> appropriate to the entire atmosphere have some distinctive properties. To begin with, air is a compressible fluid, described by the equation of state of a perfect gas for the processes of interest to us:

$$VP = RT; \quad (8)$$

here  $R$  is the gas constant. Since rising air will expand and cool, the heat equation will include an extra term<sup>5</sup>

$$w(\gamma - \gamma_a),$$

where  $w$  denotes the vertical velocity component and  $\gamma_a$  is the adiabatic gradient. In dry air the equation of continuity will be affected as well:

$$\text{div } \mathbf{v} = w \left( \frac{\gamma - R\bar{\gamma}}{RT} \right);$$

a bar designates the value in the undisturbed atmosphere, and  $\bar{\gamma} = -\partial T/\partial z$ .

If we transform to dimensionless variables in the equations of motion (2), taking the vertical side  $L$  of the region at hand as unit of length,  $L^2/\nu^2$  as unit of time, the temperature differential  $\Delta T$  between the upper and lower boundaries as unit of temperature, and  $\rho_0\nu^2/L$ ,  $\nu/L$  as units of pressure and velocity, then the system (2) will become

$$\left. \begin{aligned} \frac{\partial \mathbf{v}}{\partial t} + (\mathbf{v}\nabla)\mathbf{v} &= -\nabla P + \Delta \mathbf{v} - \text{Gr}T', \\ \frac{\partial T'}{\partial t} + (\mathbf{v}\nabla)T' &= -\frac{1}{\text{Pr}}\Delta T', \\ \text{div } \mathbf{v} &= 0, \end{aligned} \right\} \quad (9)$$

where  $\text{Gr} = |g|\beta\Delta T \cdot L^3/\nu^2$  is called the Grashof number and  $\text{Pr} = \nu/\kappa$  is the Prandtl number. The product of the Grashof and Prandtl numbers gives one other dimensionless parameter, the Rayleigh number  $\text{Ra} = |g|\beta\Delta T \times L^3/\nu\kappa$ , which expresses the ratio of the viscosity and buoyancy forces. If the buoyancy forces, as determined by the temperature gradient, are small, then the viscosity will suppress any disturbances that develop in the fluid, and motions will be damped. When the buoyancy forces reach a threshold such that viscosity can no longer damp the motions, the fluid will acquire convective flows. The corresponding  $\text{Ra}$  value is called the critical Rayleigh number; it describes the stability of the fluid against convective processes.

A nonzero critical Rayleigh number will exist only if horizontal temperature gradients are absent. When such gradients are introduced, convection motion will set in whatever the vertical temperature gradient may be.

### 3. LARGE-SCALE CONVECTIVE MOTIONS

#### a) Interlatitudinal air circulation and jet streams

The chief factor driving the movements of the atmosphere and ocean is the energy coming from the sun. Since the earth is a globe and since the tropical and polar zones differ in albedo, the energy influx is distributed nonuniformly over our planet's surface. Hence in both hemispheres the mean temperature diminishes horizontally from the equator toward the poles at all levels of the troposphere, except in layers above the 200-mb level in the tropics. As a result the air circulates interlatitudinally—a global lateral convection process. Figures 1a, b illustrate the mean winter and summer meridional circulation patterns in the Northern Hemisphere. In winter the mean flow is particularly intensive in the belt between the equator and latitude 30°N, representing the familiar Hadley tropical cell.<sup>6,7</sup>

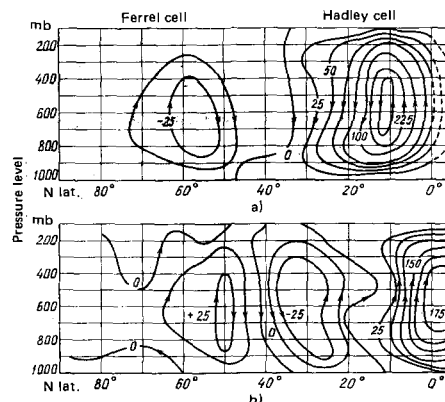


FIG. 1. The mean meridional circulation pattern in the Northern Hemisphere: a) winter; b) summer. Between each pair of adjacent streamlines  $25 \cdot 10^6$  ton/sec of air flows in the direction shown by the arrows.

In this cell, relatively light, warm air rises on the south side, and cool, dense air sinks on the north.

To the north of the Hadley cell a second, midlatitude cell has been identified, in which air moves in the opposite direction; it is called the Ferrel cell (Fig. 1). Purely physical arguments suggest that a third cell, none too well defined, ought to exist above the North Polar Zone. Such a cell is indeed present in the Southern Hemisphere, although it can also be explained by the contrast between the thermal conditions above the Antarctic continent and above the relatively warm waters of the surrounding ocean (see Fig. 4a below). We shall return to this topic in Sec. 4, when we discuss lateral convection.

In winter the total air mass circulating in the Hadley cell reaches  $230 \cdot 10^6$  ton/sec, whereas the circulation in the Ferrel cell amounts to only  $30 \cdot 10^6$  ton/sec. In summer, when the surface temperature difference between pole and equator in the Northern Hemisphere diminishes from  $50^\circ\text{C}$  to a value half as great, the Hadley cell carries the much smaller flow of  $30 \cdot 10^6$  ton/sec, while the Ferrel cell remains approximately as strong as in winter.<sup>8</sup> The most intensive meridional circulation in the northern summer turns out to result from the northward extension, beyond the equator, of the prominent winter Hadley cell of the Southern Hemisphere.

In between the Hadley and Ferrel cells, a subtropical jet stream forms in the upper troposphere. In typical cases it reaches maximum strength at the 200-mb level, and is characterized by a strong vertical wind shear. This subtropical jet represents the predominant flow in both hemispheres, particularly during the cool season.

Figure 2a, reproduced from Riehl,<sup>9</sup> indicates the axis position of the subtropical jet stream in winter. This jet flow represents a very powerful wind system around the globe; for example, speeds of 130 m/sec have been observed above Japan. It is noteworthy for its high stability in both wind direction and geographic location.

The physical process responsible for the jet streams is of outstanding interest because it involves energy transfer from small-scale motions to those of larger scale. A thorough analysis of the mechanism was first made by Starr.<sup>10</sup> At the Moscow University oceanogra-

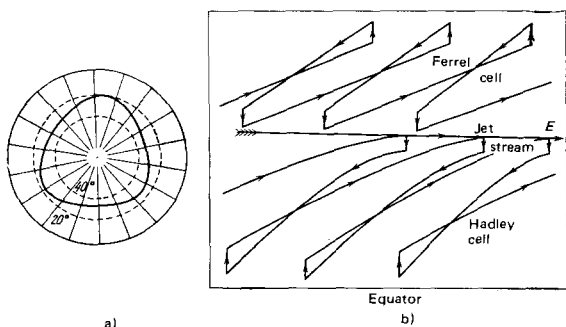


FIG. 2. a) The location of the winter subtropical jet-stream axis in the Northern Hemisphere; c) the pattern of a jet stream emerging in the atmosphere.

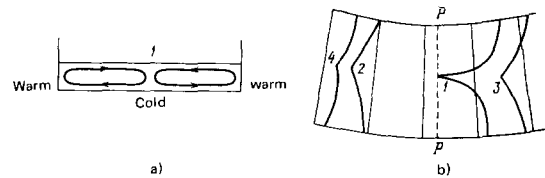


FIG. 3. Laboratory simulation of a jet stream in a ring-shaped vessel. a) A section  $pp$  across the ring, showing the convection cells; b) boundaries of spots of color distorted by the jet stream after introduction at two successive times: (1, 3), (2, 4).

phy department some experiments have been conducted which strikingly illustrate this energy-transfer process.<sup>11</sup> Into a ring-shaped vessel, its bottom chilled by dry ice, was poured a shallow (0.4 cm) layer of alcohol. The vertical temperature gradient generated a field of convection cells arranged in planes perpendicular to the horizontal plane and cutting radially across the vessel. These convective rings show up clearly when the fluid is tinted. Shortly after the experiment started one could distinctly see a jetlike flow that had developed in the surface layer. Figure 3b depicts the emergence of the jet stream as the tint substance is introduced. Notice how the spot of color changes its shape, stretching out along the axis of the ring.

Jet streams form because of the instability of opposing convective flows. In the Moscow experiments the direction of the jet was determined by the asymmetry of the disturbance produced in the fluid at initial time.

Unlike the situation in the laboratory, however, the Hadley and Ferrel convection cells in the terrestrial atmosphere are subject to a Coriolis force field; as a result, the air flow in the ground layer of a Hadley cell is deflected westward (the trade winds), but in the upper layers, eastward. In a Ferrel cell the reverse is true: the air flow is deflected westward in the upper troposphere region where the countercurrents of the Hadley and Ferrel cells interact that the jet stream develops. Its direction is controlled by the stronger Hadley circulation, with the Ferrel circulation acting as an aerial boundary (Fig. 2b).

## b) Monsoon circulation

Nonuniform heating is imparted by the sun not only to the different latitude zones around the globe but, just as much so, to oceanic and continental surfaces, and thereby to the atmosphere above.

In summer the air is warmed much faster and more strongly above land than above the sea. As a result, warm air masses shift from the continents to the ocean in the upper layers of a monsoon-type circulation, while cooler air moves from the ocean to the land at low levels. An opposite motion of air masses occurs in winter, for at that season warmer air masses form above the slowly cooling ocean than above the continents (Fig. 4). In certain cases an air circulation physically analogous to a monsoon may retain the same sign all year long, changing only in intensity. Such circulation develops above the Antarctic ice sheet and the rel-

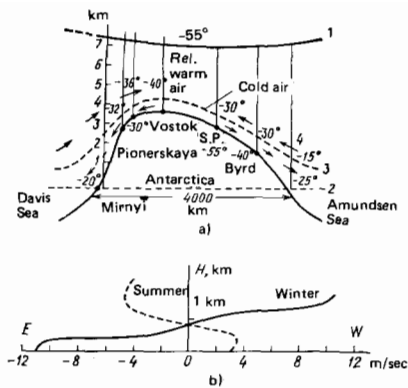


FIG. 4. a) A profile of the atmosphere above Antarctica, averaged over several years, showing the temperature in °C (1, the tropopause; 2, sea level; 3, flow interface; 4, air currents); b) height dependence of the wind velocity in a plane perpendicular to a shoreline for the Pacific Ocean monsoon.

atively warm seas surrounding it (see Fig. 4a).

The vertical profiles in Fig. 4b show the wind-velocity distribution directly above a shoreline.<sup>12</sup>

A map of the air-mass differentials above unit area of the earth's surface in January and July, prepared by Shuleikin and his collaborators,<sup>13-15</sup> testifies to the huge shortfalls of air that yawn above the oceans in the wintertime, and the humps of superfluous air mass above the continents, whereas in summer the pattern is reversed. Shuleikin<sup>13</sup> and later Dmitriev<sup>16</sup> worked out an approximate theory for this phenomenon.

### c) Mean meridional circulation in the World Ocean

As we have pointed out, the general circulation of the waters in the World Ocean is basically driven by the mechanical action of the atmosphere. The effects include gradient flows and drifts, flows induced by the to and fro thrust of the wind, and the barogradient and concomitant balancing flows. These account for (80-90)% of the kinetic energy stored in the ocean.

Thermohaline flows associated with the nonuniform density field of oceanic waters and caused by temperature and salinity differences—that is, thermal and salinity convection—generates the other (10-20)% of the ocean's total kinetic energy. Typical horizontal temperature and salinity gradients in the ocean range from tenths of a kelvin and hundredths of one percent per kilometer to an order of magnitude more.<sup>17-19</sup> Tidal ebb and flow accounts for an insignificant fraction of the energy.

In the ocean the analog to the interlatitudinal atmospheric convection is a global meridional convection. This process results from the disparity in the thermal and salinity regimes of the waters at different latitudes and from the sinking convection in the oceanic polar regions: as the deep, cold waters formed in this way warm up, they migrate toward the equator and displace the warmer waters there up to the surface, generating the portion of the convective flow directed away from the equator. Such flows are called thermohaline circulation.

An early model for horizontal thermohaline circulation was proposed by Lorenz in 1847; he recognized that waters would sink at the poles and rise at the equator. In 1908 Sandström showed experimentally that oceanic conditions are not favorable to the development of thermohaline circulation.<sup>20</sup> This result was put on a theoretical basis in 1966 by Bjerknes,<sup>21</sup> who proved that in an efficient thermal machine the heat source should be subject to higher pressure than the coolant. This condition is in fact obeyed in the atmosphere, which loses heat mainly at high levels (low pressure) and gains heat near the earth's surface (high pressure). But in the ocean heat is gained and lost chiefly in the surface layers, at even pressure.

In 1950 Stommel investigated the rates of flow resulting from the unequal warming of waters in different parts of the World Ocean, and found the rates to be small.<sup>22</sup> Stommel also showed that thermohaline flow can explain certain important features of the global circulation of oceanic waters. By analyzing diagrams for the depth profiles of temperature and salinity [ $T, S$  diagrams] down to 4 km, he demonstrated that in the polar regions the ocean contains two comparatively limited zones of sinking surface waters, where cold water runs at deep levels. One of these occurs in the North Atlantic ( $T = 2^\circ\text{C}$ ,  $S = 34.9\%$ ), the other in the Weddell Sea off Antarctica ( $T = 0^\circ\text{C}$ ,  $S = 34.7\%$ ). The process creates two deep, cold streams flowing toward the equator, and corresponding warm surface currents flow from the equator toward the polar regions. Calculations indicated that these sources are of about the same strength, with a flow equal to about 20 sverdrups ( $1 \text{ Sv} = 10^6 \text{ m}^3/\text{sec}$ ), and are comparable with the flow rate of the great ocean currents (Gulf Stream, 30 Sv; Antarctic West Wind Drift, 200 Sv). This superposition of thermohaline circulation upon wind-driven flow was shown by Stommel to explain the asymmetry of the westerly surface flows in the Atlantic Ocean. In the Northern Hemisphere the northward surface branch of the thermohaline flow reinforces the Gulf Stream; in the Southern Hemisphere the surface branch flows southward, against the Brazil current, thereby weakening it. The model predicted that beneath the Gulf Stream should be a cold countercurrent. That current was discovered<sup>23</sup> in 1958.

The meridional circulation of Atlantic waters is distinctly shown by the profiles in Fig. 5.<sup>24</sup> A similar circulation pattern is observed in the Pacific Ocean.

Many authors have investigated the large-scale thermohaline flows.<sup>25-31</sup> All these studies have a common feature: the mathematical models treat the process as

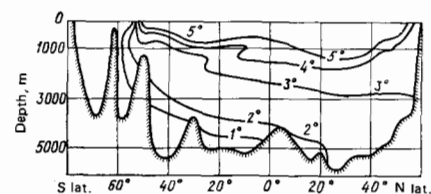


FIG. 5. Temperature profiles [°C] along a quasi-meridional section of the West Atlantic (after Nekrasova and Stepanov<sup>24</sup>).

quasisteady. The vertical component of the motion has been determined from the continuity condition, so that convection is not taken directly into account. Such model solutions are valid only for regions distant from the formation sites of the vertical currents; they are more suitable for diagnosing than for predicting the phenomenon. The same is true of the analogous models for the atmosphere.

The examples we have given of large-scale atmospheric and oceanic motions are typical instances of lateral convection, which can be described accurately only by the system of equations (1). In pure form such convection will develop only in a stably or neutrally stratified fluid whose density varies horizontally. As we shall see presently, numerical solutions of the system (1) for various cases of vertical Rayleigh convection, where the liquid or gas volumes are considered to have a near-unity ratio of height  $H$  to horizontal scale  $l$ , have shed light on many aspects and properties of this convection process.

To some extent a similar approach can be taken to cases of lateral convection that develops in applied contexts when  $H/l \gg 1$ , that is, in narrow vertical slits. But in geophysics we know that lateral convection typically has  $H/l \ll 1$ , the convection cells being much elongated in a horizontal direction. The capabilities of solving such problems numerically are still very limited, especially if they are three-dimensional. It also is a complex task to study convection processes in nature. That is why much of the analysis has had to be done in the laboratory, particularly with rotating-fluid simulations. Another reason is that a general proof has yet to be given for the theorem that the solution of the Navier-Stokes equations is unique. To be sure, the doubt would remain even if numerical solutions were obtained. Approximate analytic solutions to the linearized equations have been used as well. In fact hundreds of papers have now been published on this subject.

Convection in a rotating fluid was first studied by Fultz,<sup>32</sup> Hide,<sup>33</sup> and Bonchkovskaya.<sup>34</sup> In 1953 Starr and Long proved the similarity of these models to natural phenomena.<sup>35</sup> The extensive research since that time has been summarized in several reviews.<sup>36-38</sup>

The key factors influencing the convection regime have turned out to be the heating and rotation of the fluid. Either of two regimes will be realized, depending on these factors: a) Hadley convection, with axisymmetric motion; b) Rossby convection, with the axisymmetric regime perturbed by waves. The changeover from one regime to the other occurs for a particular angular velocity and heat influx, and is determined by the critical Taylor number.<sup>39-41</sup>

In the ocean and other basins—seas, lakes, reservoirs—lateral convection can also develop within relatively small volumes, when the rotating-fluid effects may be neglected. Here too there has been much research. A typical model has been the convection that arises in a rectangular vessel whose end walls are heated unequally. The mathematical treatment has been limited to the two-dimensional problem. Studies of this

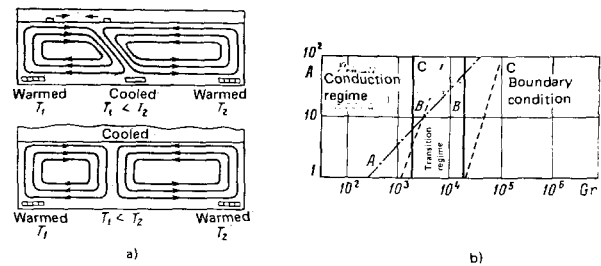


FIG. 6. a) Water currents in rectangular aquaria subject to different boundary thermal conditions<sup>42</sup>; b) lateral-convection regimes in a fluid (line A separates the conduction and transition regimes; lines B and lines C bound the regimes with Prandtl number  $Pr \approx 1$ ; ordinate, vessel height/length ratio; abscissa, Grashof number).

kind are also valuable because they permit detailed analysis of how boundary conditions affect the convection regime; to do that in the three-dimensional problem with rotation would be much harder.

In nature, in both the atmosphere and the ocean, convection will often set in when conditions along the horizontal boundaries are none too clear; and generally speaking the vertical boundaries will not be very definite, since there are hardly any rigid walls. It is customary in these cases to take as boundaries the midlines of the rising or descending streams in two contiguous convection cells. In 1946 one of the authors<sup>42</sup> investigated the behavior of these boundaries experimentally, using sources of heating and cooling of differing intensity. The interface between the cells in some cases shifted along with the descending flow, remaining vertical; in other cases it merely tilted, without breaking away from the heat source (Fig. 6a).

Lateral convection, unlike vertical convection, can be triggered by arbitrarily small departures from an equilibrium density distribution.<sup>43</sup> Over a wide range of Rayleigh numbers  $Ra$ , the lateral-convection cell size is equal to the horizontal scale of density irregularity. At certain  $Ra$  values, sufficiently elongated cells will begin to split into an odd number of smaller cells. Probably this is what causes the breakup of the interlatitudinal circulation cells, which encompass one-quarter the length of a meridian.

The ill-defined character of the third, polar, interlatitudinal circulation cell in the Northern Hemisphere, and conversely its prominence in the Southern Hemisphere, may be attributed to the distinctive thermal regimes of the underlying surface in these regions. In the south, the interlatitudinal contrast of the surface thermal regime is aggravated in the polar regions by the contrast between the Antarctic ice cap and the relatively warm waters around it. In the Northern Hemisphere the interlatitudinal contrast and the land-sea contrast have opposite signs, weakening the third, polar, cell.

At the same time, however, large cells will be stabilized by rotation, as we shall see when we discuss convection in a centrifugal force field, taking the atmosphere as an example.

Before describing briefly the research on lateral free convection in nonrotating rectangular basins, we would emphasize the difference between vertical and lateral convection in terms of size and cell regime. Blinkov and one of us have shown<sup>44</sup> that unlike the case in lateral convection, when a convection cell develops vertically its size will depend on the Grashof number, diminishing as  $Gr$  increases.

Both theoretical and laboratory studies have demonstrated<sup>45,46</sup> that the lateral convection regime is determined mainly by three dimensionless parameters:  $Gr$ , the Prandtl number  $Pr$ , and the height/length ratio  $H/l$  of the vessel. The following three lateral-convection regimes have been identified by experiment<sup>47,48</sup>:

a) The conduction regime, when thermal conductivity transfers heat from the warm to the cool wall. A constant temperature gradient is established in the interior; the local Nusselt number  $Nu$ , measuring the heat flow across the cool vertical wall, depends only on  $Gr$ , not on  $H/l$ .

b) The transition regime, characterized by a nonlinear horizontal gradient and by weak convection in the interior of the fluid.

c) The boundary-layer regime, in which a nucleus develops inside the fluid, surrounded by boundary layers (vertical and horizontal boundaries). If the Rayleigh number is large enough ( $Ra \gg 10^3$ ), a stationary nucleus will form within the fluid, its temperature varying vertically.

These experiments have been confirmed by numerical analysis.<sup>45,49-51</sup> Others have also studied the flow structure<sup>52,53</sup> for  $H/l \gg 1$ . Experiments and numerical calculations have now established<sup>54</sup> that for basins having  $H/l > 1$  the  $Gr$  values delimiting the transition regime are independent of  $H/l$ ; for the conduction regime  $Gr \ll 2.2 \cdot 10^3$ , while in the boundary-layer regime  $Gr \gg 2.9 \cdot 10^4$  (Fig. 6b).

Some cases of lateral convection with  $H/l \ll 1$ , the situation more pertinent to geophysics, have been investigated,<sup>55-57</sup> but there have been only a few such studies. They neglect the influence of stratification in the fluid upon the convection regime, they do not adequately consider how the thermal and dynamical conditions along the horizontal boundaries affect the flow regime in the interior for large  $Ra$  values (the boundary-layer regime), and the dependence of the convection regime upon salinity has not yet been thoroughly explored.

To a limited degree these matters have recently been considered by Blinkov and one of us.<sup>58-60</sup> An approximate analytic solution to the linearized equations (1) describing the regimes in different parts of a convection cell yields the following results:

1. For the convection excited by unequal warming of the side walls of a basin at small  $Ra$  values, we find that if the temperature of a side wall is variable, the layer formed next to it will result from a more delicate balance of forces than if the side-wall temperature remains constant, and will contain two transition regions. In the outer transition layer the horizontal velocity

field within the basin accommodates itself to the seal imposed by the wall; vertical transfer of heat and mass is concentrated in that zone. In the inner transition layer the thermal regime of the outer zone adjusts to the heating of the basin side walls. For the case of lateral convection in horizontally distended basins, the changeover from the conduction regime to the transition regime is accompanied by a transformed horizontal structure of the convection cell; when the transition regime goes over to the boundary-layer regime, the vertical flow structure in the inner side-wall zone is altered.

2. Salinity manifests itself by a substantial change in the convection dynamics. First, the temperature profile in the fluid and the factors controlling it are different in salt water than in fresh; second, the boundary layers play a different role. Physically, these changes mean that  $Nu$  will be independent of  $Ra$  for the large  $Ra$  values found in salt water.

If two bodies of ocean water, one warm and salty, the other cool and less salty, should mix convectively, regions may form with a vertical temperature inversion. An estimate has also been made<sup>58-60</sup> of the amplitude of the vertical temperature differential in the nucleus that may develop through convection.

Even in basins spread out horizontally, lateral convection has been studied under conditions not quite the same as found in nature. Nevertheless, the results obtained may be applicable to a variety of geophysical problems, such as estimating the size of the rising and sinking flow regions within which the quasisteady approximation is untenable, and also determining the thermal and dynamical regimes in these convection regions.

One other contributor to the oceanic circulation is the flow of moisture carried through the atmosphere. Although the amount involved is not so great as in the liquid water currents at the surface, it still is appreciable. The trade winds, for example, transport 0.1 Sv of moisture. Thus they help exchange water between the Pacific and Atlantic Oceans.

#### d) Mantle convection

The question of whether the whole mantle of the earth is caught up in large-scale convective motion continues to arouse lively debate among theoretical geophysicists.<sup>61-67</sup> In many respects this is inevitable, because we have only indirect evidence for a number of the quantities describing the interior of the earth.

Applying general methods of similarity and dimensionality theory, Golitsyn<sup>65</sup> has been able to estimate the convective velocities in the mantle. He describes the convection by the Boussinesq approximation to the equations of hydrodynamics. A significant role is played by viscous dissipation at a rate

$$e = \nu \frac{\partial v_i}{\partial x_k} \left( \frac{\partial v_i}{\partial x_k} + \frac{\partial v_k}{\partial x_i} \right), \quad (10)$$

where the kinematic viscosity  $\nu = 2 \cdot 10^{17}$  m<sup>2</sup>/sec; the  $v_i$  are the velocity-vector components, and summation over repeated indices is understood. Because of this

enormous viscosity the convection of mantle material is laminar, and the heat flux from the core at the lower boundary is converted into mechanical energy with fairly high efficiency. All this energy is once again dissipated as heat, in accord with Eq. (10). The mean rate of heat output per unit mass of mantle material is  $q = f/\rho d$ , where  $f$  denotes the heat flux density across unit surface area (the mean geothermal heat flow amounts to  $0.06 \text{ W/m}^2$ ),  $\rho = 3.7 \text{ g/cm}^3$  is the density of the mantle material, and  $d$  is the mantle thickness. In a steady state, kinetic energy would be generated at a rate  $\varepsilon = \gamma q$ , where  $\gamma$  is the efficiency with which the convective flow transforms the heat into mechanical energy. Equation (10) may now be written as

$$\frac{\gamma f}{d\rho} \sim v \cdot 16 \left( \frac{2U}{d} \right)^2,$$

whence we obtain

$$U \sim \frac{d}{4} \sqrt{\frac{\gamma q}{2v}}. \quad (11)$$

Taking  $\gamma = 1$  and  $d = 700 \text{ km}$  we find a flow speed  $U = 5 \text{ cm/yr}$ . This value is comparable with the drift rate of the lithospheric plates,  $1\text{--}10 \text{ cm/yr}$ , so the convection efficiency should be quite high.

One can obtain another expression for the mean convective flow speed  $\bar{U}$ , analogous to Eq. (11), by analyzing the system of dimensionless Boussinesq equations for the convection to find their range of applicability and to derive the basic similarity criteria needed for laboratory simulation.

The mantle problem has a Reynolds number  $Re \approx 10^{-22}$ , so one may neglect the nonsteady and inertial terms. Straightforward operations then yield the relation

$$\Delta \text{rot } U = F [\nabla T n],$$

where the parameter  $F = \alpha T_0 g d^2 / \nu u$  (the thermal expansion coefficient  $\alpha = 2 \cdot 10^{-5} \text{ }^\circ\text{K}^{-1}$ ,  $g = 10 \text{ m/sec}^2$ ,  $T_0$  is the characteristic temperature at a certain depth) and  $n$  is the unit vector along the force of gravity.

In turn the number  $F = Ra / Pe$ , where  $Ra$  is the Rayleigh number. The Péclet number  $Pe$  specifies the strength of the *advective* heat transfer (macrotransfer in a horizontal direction) relative to the molecular transfer. In the process at hand  $Pe \approx 700$ , so that molecular heat transfer is insignificant compared with advection. If  $T_0 = 1500 \text{ }^\circ\text{K}$ , the number  $F \approx 500$ . The quantity  $qd/UC_p T_0$  occurring as a coefficient in the first term on the right in the energy equation describes the distribution of heat sources and viscous dissipation; it acts as a similarity parameter  $\mu$  specifying the heat released in a column of mantle material during a time span  $\tau_0 = d/U \approx 15 \cdot 10^6 \text{ yr}$ . Since  $\Gamma \gg 1$ ,  $\mu \ll 1$ , and  $Pe \gg 1$ , the similarity conditions may be assumed satisfied—a very important factor in laboratory simulations.

This approach also enables the efficiency  $\gamma$  to be evaluated for various modes of heat influx into the convective system. It turns out that  $\gamma$  depends little on the particular input mode and is  $\approx 10\%$ . By comparison, the solar heat entering the atmosphere is transformed into wind kinetic energy with  $\approx 1\%$  efficiency.

It is unlikely, though, that pure thermal convection

takes place in the mantle. Probably the convection is of density-chemical character: the main source of motion should be density fluctuations in the material that result from changes in its chemical composition by differentiation. The onset of convection will then be described by a different criterion, the Rayleigh number taking the form

$$Rg = \Delta \rho g \frac{H^3}{D \eta},$$

where  $D$  is the diffusion coefficient. Estimates indicate that in the lower mantle  $Rg$  will have a value somewhere in the range

$$10^{17} < Rg < 10^{34},$$

many orders of magnitude above the critical value.

The only way properly to describe the influence of upper-mantle density irregularities on the development of convective motions in the terrestrial envelope is by computer simulation of the density-chemical convection process.<sup>62</sup>

If horizontal irregularities occur in the mantle, and if it has the properties of a Newtonian fluid, then large-scale lateral convection may develop as well, with a cell size equal to the scale of horizontal inhomogeneity. Such convection will be even more likely if it can set in for an arbitrarily small Rayleigh number. Large-scale cells may also form in a homogeneous density field, as suggested by calculations of the convection in a centrifugal force field (Sec. 3f) as well as by Chandrasekhar's theoretical research.<sup>61</sup>

### e) Atmospheric convection induced by motion of terminator<sup>1)</sup>

We have been discussing the meridional and land-sea temperature gradients as mechanisms for triggering convective motion. Lately, however, increasing attention has been accorded the "heat machine" associated with the diurnal temperature variation in the atmosphere.

That the heat flux induced by the diurnal temperature wave might contribute to the global circulation of the atmosphere was first suggested by the British astronomer Edmund Halley nearly 300 years ago.<sup>68</sup> In particular, this hypothesis regards the easterly trade winds in the earth's equatorial belt as caused by the diurnal temperature wave, rather than by the deflection of the meridional Hadley-cell flow due to the earth's rotation.

The first experiment to test this idea was that performed by Fultz *et al.*,<sup>69</sup> who moved a Bunsen burner flame in a circle below the edge of a stationary cylindrical vessel containing water. The moving heat source set the water surface moving in the opposite direction, but on the bottom of the vessel a motion was observed in the same sense as the motion of the flame. The measured speed of the surface counterdrift was less than 1% that of the moving flame. At nearly the same time, similar experiments were conducted by Stern.<sup>69</sup>

<sup>1)</sup>The terminator is the dividing line between the dark and sunlit parts of the earth's surface.

These experiments established that a traveling heat wave will induce weak currents, and qualitatively supported the belief that Halley's hypothesis concerning the terrestrial atmosphere was correct.

With the swift progress of space technology, data have been acquired for other planets which show that the flows induced by the moving heat source may play an important role in their atmospheres. For instance, radar observations have determined for Venus a rotation period of  $244 \pm 2$  days, but the clouds in the upper Venus atmosphere rotate<sup>70</sup> in only  $4.3 \pm 0.4$  days. Schubert and Whitehead<sup>71</sup> offered an explanation based on the dynamical relationship of the vertical convection in the Venus atmosphere to the radial flow induced by the solar heat wave; the flow would move in the opposite direction. Repeating Stern's experiment, they used mercury as the working fluid because of its high thermal conductivity. The surface countercurrent that developed was four times faster than the revolving burner.

The inducement of direct and retrograde flows in a fluid by a traveling thermal wave may be explained qualitatively as follows. Consider a fluid layer of infinite extent. Then if  $Re$  exceeds a critical value, convection currents will be set up in the fluid. A temperature wave moving beneath the vessel will, by its extra heating, tend to displace the rising fluid elements along its direction of motion. The convection cells will tilt, and if  $Re$  is large enough a velocity component will develop in the top layer opposing the motion of the thermal wave. This component will result from the interaction of the vertical currents at the upper boundary. Similarly, currents will be generated near the lower boundary moving opposite to the thermal wave.

This phenomenon has now been described in a number of theoretical studies.<sup>72-74</sup> The basic idea in solving the problem is to average the equations of vorticity and heat conduction, written in the Boussinesq approximation, with respect to the length and period of the temperature wave. In all cases it has been assumed that  $\lambda \gg H$ , the length of the temperature wave much exceeding the thickness of the fluid layer in which convection develops. If the viscosity is so low that the Prandtl number  $Pr = \nu/\kappa \ll 1$ , the mean speed of the current will be proportional to the quantity

$$\bar{u} \sim F^2 \sqrt{Ra},$$

where the dimensionless parameter

$$F = \frac{gH}{U^2} \frac{\Delta\rho}{\rho}$$

measures the intensity of the effect due to the temperature wave;  $U$  is the linear velocity of the temperature pulse, and the Reynolds number is  $Re = H^2/\nu t$ , with  $t$  the period of the temperature wave. The expression for  $\bar{u}$  shows that if the vertical convection speeds are high enough, a mean flow can be generated whose velocity is comparable with that of the thermal wave.

For six planets in the solar system, Table I gives values<sup>72</sup> for the heat flux  $q$  from the sun, the equatorial velocity  $U$  of the terminator, the mean thermal-action parameter  $\bar{F}$ , and the frequency parameter  $Re$ . We see

TABLE I. Planetary thermal parameters.

Planet	$q, \frac{\text{erg}}{\text{cm}^2 \cdot \text{sec}}$	$U, \text{m/sec}$	$\bar{F}$	$Re$
Venus	$6.3 \cdot 10^8$	3.0	$10^2$	$10^2$
Earth	$8.4 \cdot 10^8$	$4.7 \cdot 10^2$	$10^{-2}$	$10^4$
Mars	$5 \cdot 10^8$	$2.8 \cdot 10^2$	$10^{-3}$	$10^4$
Jupiter	$2.5 \cdot 10^8$	$1.2 \cdot 10^4$	$10^{-6}$	$10^4$
Saturn	$7.6 \cdot 10^8$	$1.0 \cdot 10^4$	$10^{-7}$	$10^4$
Uranus	$1.2 \cdot 10^9$	$3.7 \cdot 10^3$	$10^{-7}$	$10^4$

that Venus has a thermal-action parameter four or five orders larger than any other planet, so its atmosphere will respond the most strongly to the periodic influx of heat.

On Mars we observe strong winds blowing in the same direction that the terminator moves. But they cannot be attributed to the mechanism outlined above: it would imply a velocity many orders lower. More than 75% of the Martian atmosphere is carbon dioxide<sup>74</sup> which, by absorbing and emitting infrared radiation, does little more than alter its own internal energy. Hence the Martian atmosphere has a much lower thermal inertia than the earth's atmosphere, and the diurnal temperature variations of the planetary surface are conveyed into the atmosphere by radiation to heights of several kilometers. Accordingly the atmosphere of Mars is characterized by substantial diurnal temperature fluctuations and a higher rotational velocity than on Venus.

Since radiative transfer will establish thermal equilibrium practically instantaneously in the Martian atmosphere, depending on the time of day, it is interesting to study how a flow will develop in a fluid when gravitational forces are absent. At Moscow University the authors and colleagues have considered a mechanism for inducing such convection.<sup>75</sup>

Suppose that a zone of length  $L$  with an enhanced temperature  $T_2$  is moving at a constant speed  $\omega_T$  in a given direction through a long, thin ring tube filled with fluid (Fig. 7a). At the ends of zone  $L$  apply a heat source  $H$  and a coolant  $C$ , producing pressure differentials  $P_{H^+} - P_{H^-}$ ,  $P_{C^-} - P_{C^+}$  at the two respective boundaries. Assume that the fluid inside the regions of constant temperature  $T_2$ ,  $T_1$  is incompressible, and that Poiseuille flow is taking place with mean velocities  $u_1$ ,  $u_2$  in regions 1, 2.

We are to determine the value and direction of the flow velocities in regions 1, 2 and the mean flow vel-

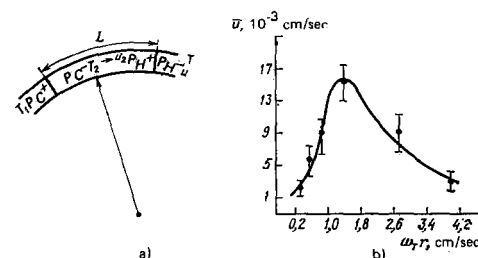


FIG. 7. a) The slow-heating model configuration; b) an experimental curve for the dependence of the mean direct-drift speed on the rotation speed of the heat source.

ocity. For this purpose we write the equation of mass conservation, the equation of continuity for the momentum flux, the Poiseuille law, and the equations of state for the two regions:

$$\left. \begin{aligned} (u_1 - \omega_1 r) \rho_1 &= (u_2 - \omega_2 r) \rho_2, \\ P_{H^-} + \rho_1 (u_1 - \omega_1 r)^2 &= P_{H^+} + \rho_2 (u_2 - \omega_2 r)^2, \\ P_{C^+} + \rho_2 (u_2 - \omega_2 r)^2 &= P_{C^-} + \rho_1 (u_1 - \omega_1 r)^2, \\ \frac{P_{H^-} - P_{C^+}}{2\pi r - L} &= \frac{8\mu}{R^3} u_1, \quad \frac{P_{C^-} - P_{H^+}}{L} = \frac{8\mu}{R^3} u_2, \\ \rho_1 &= \rho_0 (1 - \beta T_1), \quad \rho_2 = \rho_0 (1 - \beta T_2). \end{aligned} \right\} \quad (12)$$

We introduce the notation

$$\frac{2\pi r - L}{L} = Y, \quad \frac{\rho_2}{\rho_1} = 1 - X.$$

When  $X = 0$ , no heating takes place; when  $X = 1$ ,  $T_2 \rightarrow \infty$ , and the heated region takes on the properties of a piston. Equations (12) yield the flow velocities

$$u_1 = \frac{\omega_1 r X}{1 + Y(1 - X)}; \quad u_2 = \frac{-\omega_2 r X Y}{1 + Y(1 - X)}. \quad (13)$$

We have not yet made use of the equation of state. In real processes the interface at the heat source will have a finite size, and  $T_2$  will not be reached instantaneously, so we may write

$$\frac{dT_2}{dt} = \xi (T_{\max} - T_2),$$

whence

$$T_2 = T_{\max} (1 - e^{-\xi L / \omega_2 r}) = T_{\max} Z,$$

and

$$X = 1 - \frac{\rho_2}{\rho_1} = \beta T_2;$$

the constant factor  $\xi$  characterizes the properties of the material in the tube. The flow velocity averaged over the length of the tube is then found to be

$$\bar{u} = \frac{\omega_1 r (\beta T_{\max} Z)^2}{(1 - \beta T_{\max} Z) Y + (1/Y) [(1 - \beta T_{\max} Z)^2 + 1]}.$$

Figure 7b plots the experimental values for the mean rate of direct drift as a function of the speed of the rotating heat source.

Now we can make some rough estimates of the mean flow velocity induced in the atmospheres of Venus, the earth, and Mars. These values are given in Table II. On Venus the night and day temperatures of the upper atmosphere differ anomalously ( $T_n > T_d$ ); hence the parameter  $X > 1$ , contrary to the conditions of the "slow heating" model discussed above (cf. Table II).

From the comparisons in Table III it is clear that the model best fits the Martian atmosphere: the computed and measured wind velocities are approximately the same. Moreover, the mean eastward flow velocity obtained in the slow-heating model agrees in value and direction with the results of numerical simulations<sup>76,77</sup>

TABLE II. Planetary diurnal heating.

Planet	Measured temperature		Place measured	$\omega_1 r$ , m/sec	$X$
	$T_{\text{night}}$ , °K	$T_{\text{day}}$ , °K			
Venus	242	233	Equator, upper atmosphere	3	1
Earth	298	299	Equator above sea	$4.7 \cdot 10^2$	0.1
Mars	190	270	Latitude zone $-20^\circ < \varphi < 40^\circ$ , in clean atmosphere above surface	$2.8 \cdot 10^2$	0.3

TABLE III. Planetary winds.

Planet	Measured wind velocity	Mean velocity resulting from Halley's convection mechanism	Mean velocity predicted by slow-heating model
Venus	-(60-140) m/sec, upper atmosphere	-100 m/sec	-
Earth	+2.5 m/sec, lower atmosphere, trade-wind zone	weaker than -0.01 m/sec	+1.25 m/sec
Mars	+10 m/sec, above surface at latitude $-24^\circ$	-	+11 m/sec

for the predicted Martian wind regime in the zone of intensive insolation,  $-20^\circ < \varphi < +40^\circ$ .

### f) Convection in centrifugal force field

So complex are the processes in the terrestrial atmosphere that in addition to analyzing the atmospheric dynamics equations one is compelled to build physical models in order to study certain aspects of the circulation. Naturally the more regular atmospheric processes are most readily simulated. For example, measurements of the air circulation in Antarctica, where the Coriolis force field and the latitudinal temperature differentials of the underlying surface are mutually symmetric, have prompted a series of experiments to investigate eddy formation in rotating ring-shaped and round basins heated in various ways.<sup>78-81</sup> In all these experiments, just as in nature, centrifugal forces have necessarily been present. Accordingly it is also worthwhile to treat the problem of thermal convection in a centrifugal force field from a theoretical viewpoint. Solutions to such problems are in fact of independent interest for studies of baroclinic instability.

Akimova and the authors<sup>82</sup> have considered the motion of a viscous, incompressible, heat-conducting fluid confined between a pair of infinite coaxial cylinders rotating at the same angular velocity  $\Omega$ . A constant temperature differential  $T_2 - T_1$  is maintained between the cylinders, with heat applied at the outer cylinder. The analysis is limited to a layer shallow enough for vertical motions to be neglected.

In a rotating coordinate system the process of convective motion in the fluid will be described by the following set of thermohydrodynamic equations, written in the Boussinesq approximation:

$$\left. \begin{aligned} \frac{\partial \mathbf{v}}{\partial t} + (\mathbf{v} \nabla) \mathbf{v} &= -\frac{\nabla P}{\rho_0} + \tilde{\nu} \Delta \mathbf{v} - 2[\Omega \mathbf{v}] + \beta T [\Omega [\Omega \mathbf{r}]], \\ \frac{\partial T}{\partial t} + (\mathbf{v} \nabla) T &= \chi \Delta T', \\ \text{div } \mathbf{v} &= 0. \end{aligned} \right\} \quad (14)$$

Here  $\mathbf{v}(r, \theta, t)$  is the velocity vector,  $\rho_0$  denotes density,  $\beta$  is the thermal expansion coefficient,  $\tilde{\nu}$  is the turbulent viscosity coefficient,  $P(r, \theta, t)$  represents the deviation of the pressure from its equilibrium value,  $T'(r, \theta, t)$  is the deviation of the temperature from equilibrium, and  $\chi$  is the thermal conductivity coefficient of the fluid.

One can obtain conditions for mechanical equilibrium of the fluid by solving the system (14) for  $\mathbf{v}(r, \theta, t) = 0$ . In a steady state the temperature and pressure will have the equilibrium values

$$T_0(r) = \frac{\ln(r/r_0)}{\ln(R/r_0)} (T_2 - T_1) + T_1,$$

$$\nabla P_0(r) = -\rho_0 [\Omega^2 r],$$

where  $T_1$ ,  $T_2$  are the temperatures of the inner and outer cylinders.

The equation of continuity implies that a stream function exists such that

$$v_r = \frac{1}{r} \frac{\partial \psi}{\partial \theta}, \quad v_\theta = -\frac{\partial \psi}{\partial r}.$$

Applying the curl operator, we may write the equation of motion in the form

$$\frac{\partial \Delta \psi}{\partial t} + \frac{1}{r} \left( \frac{\partial \psi}{\partial \theta} \frac{\partial \Delta \psi}{\partial r} - \frac{\partial \psi}{\partial r} \frac{\partial \Delta \psi}{\partial \theta} \right) = \Delta \Delta \psi + Gr \frac{\partial T}{\partial \theta}. \quad (15)$$

By solving the system of equations obtained in this way for the stream function and the temperature, assuming that the adhesion and impermeability conditions hold at the inner and outer cylinder boundaries, one can find the equilibrium convection pattern that becomes established in the centrifugal force field. The process is depicted in Fig. 8. We find here a pattern qualitatively resembling the processes observed both experimentally<sup>78-81</sup> and in the atmosphere above Antarctica.<sup>83-85</sup>

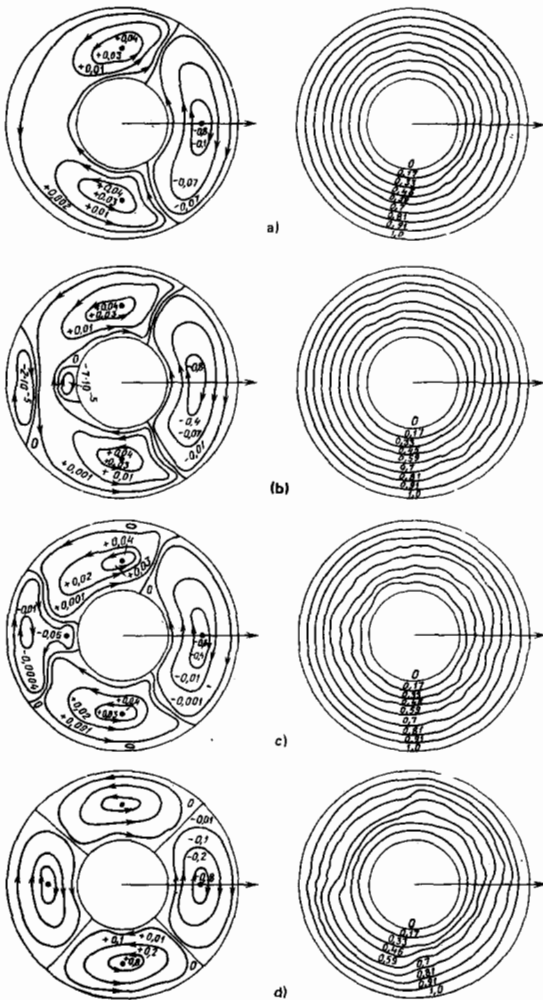


FIG. 8. Successive steps whereby the stream function and temperature between a pair of unequally heated rotating cylinders reach a steady state.

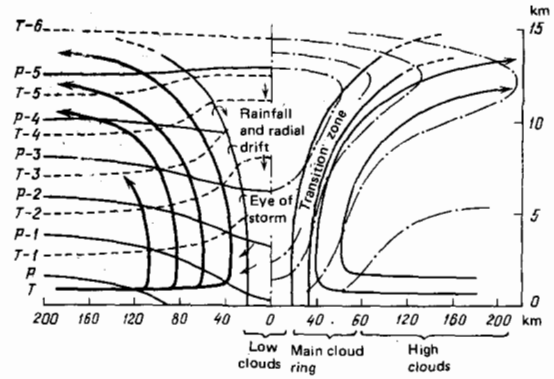


FIG. 9. The structure of a tropical cyclone.

#### 4. MEDIUM- AND SMALL-SCALE CONVECTION

a. One example of a convective system of intermediate scale is a tropical hurricane. Figure 9 illustrates the structure of a hurricane schematically. A mature system can be subdivided into four zones: 1) an outer region, bounded by convection, where the wind velocity increases toward the center; 2) a hurricane wind belt in the interior of the disturbance, with squalls and strong convection; 3) an inner region of precipitation (the wall of the eye of the storm), more or less ring-shaped, with heavy downpours and squalls of peak velocity; 4) the eye of the storm, where the winds slacken greatly as the center is approached.

Most tropical cyclones are somewhat asymmetric, mainly because of their translational motion. To a first approximation, however, one may adopt a quasisymmetric toroidal circulation to treat the principal aspects of tropical cyclones. The earliest mathematical models therefore described tropical cyclones as axisymmetric convective systems.<sup>8</sup> Recently some three-dimensional numerical models of these convective vortices have been worked out.<sup>86, 87</sup>

Tropical cyclones are convective eddies measuring 200–800 km across. They develop only above the ocean, with its abundance of vaporizing moisture, as the latent heat transported by the convection into the upper air layers makes a decisive contribution to the energy budget of the cyclone. The lowest temperature at which a cyclone has a good chance to form is 26–27°C. Since the Coriolis force stabilizes the developing vortex disturbances, the Coriolis parameter  $2\Omega \cos \varphi$  ( $\Omega$  is the earth's angular rotational velocity,  $\varphi$  is the latitude) should exceed some optimum value, thereby precluding the formation of tropical cyclones in a 5° zone on either side of the equator.

Other instances of medium-scale lateral convection in the atmosphere include breeze circulations and, over the ocean, the lateral convection induced by intermediate-scale irregularities in the surface thermal and density regime, or by the convergence of water masses differing in density. To a limited extent, some of the theoretical and experimental results for lateral convection discussed in Sec. 3 are pertinent here as well.

A convective thundercloud represents an atmospheric process in between the medium and small scales. The

horizontal diameter, ranging from several kilometers to 1 km or even less, brings the thundercloud close to small-scale phenomena, but in vertical extent, up to 7 km, it approaches the processes of medium scale. Some years ago Lebedev<sup>88</sup> developed a mathematical model for a thundercloud.

b. During anticyclone conditions close to midday in summer, when sizable areas of the continents and oceans are warmed uniformly, a rather mild convection is set up in the atmosphere above, producing a characteristic convective low-level cloud deck. This is a typical case of fine-scale convection in the atmosphere. Satellite photographs of such clouds show that the regular cells of the cloud system resemble Bénard convection.<sup>89</sup> Our group has been studying the mechanism responsible for that convection.<sup>90</sup>

At a height of about half a meter in the driving layer of air above the oceans, a temperature inversion is often observed. Khundzhua *et al.*<sup>91,92</sup> have shown that the inversion is associated with a volume heat source which develops in this layer. The source results from the mixing of dry air with the water vapor coming off the ocean surface by weak convection and turbulent exchange.

The diurnal cycle in the horizontally uniform thermal conditions on the ocean surface, when the temperature differential between air and water changes sign, induces a distinctive convection in the surface water layer. Numerical solutions of Eqs. (1) for this problem indicate<sup>93</sup> that vertical circulation cells with a horizontal axis will develop, with opposing motion in adjacent cells (Fig. 10a). In these calculations the exchange coefficient has been set equal to a suitable turbulent coefficient.

Sporadic fluctuations in the air temperature and the salinization of the water through evaporation produce a fine-scale sinking convection in the upper layers of the

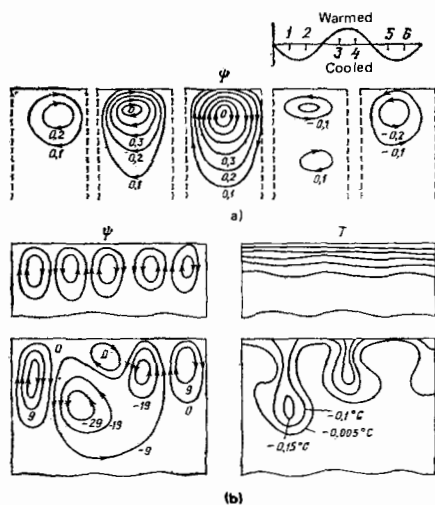


FIG. 10. Fine-scale convection in the oceanic surface layer. a) Periodic convection structure caused by the diurnal changes in the surface temperature ( $\psi$  is the stream function); b) the onset of convection in water cooled from above ( $\psi$  and temperature  $T$ ).

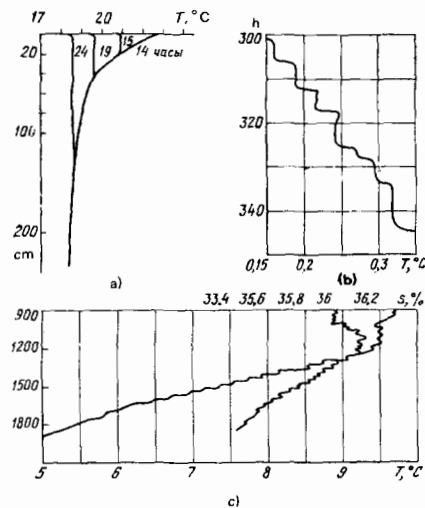


FIG. 11. a) Temperature-depth profile in a laboratory simulation of the penetrating-convection process<sup>94</sup>; b) a typical stepped thermal structure associated with the stratified convection in a temperature inversion layer in the Antarctic basin; c) step structure accompanying the "salt fingers" from Mediterranean waters entering the Atlantic.

ocean within a quasihomogeneous stratum whose thickness, 30–80 m, is largely determined by that convection. Figure 11a illustrates the temperature variation process observed experimentally when convective chilling is introduced.<sup>94</sup> This experiment was conducted with the ETEKOS facility at Moscow State University. A stably stratified temperature profile was first produced by warming the water from above. Then the cooling system was turned on. The chill gave rise to an isothermal layer.

In the ocean, where the surface warming and cooling process, though small in scale, is horizontally nonuniform, the local hydrostatic instability results in underflow or downwelling processes (small-scale lateral convection). One gains the picture of an ocean that nearly everywhere forms a fine-stratified medium containing layers of relatively uniform properties, from tens of meters to tens of centimeters thick, separated from one another by thin interface lamellae with abrupt changes in thermohaline parameters.<sup>95</sup> In Figs. 11b, c we show samples of the step structure associated with the density-type convection that develops as the salinity varies.

It is a more difficult matter to calculate numerically the temperature variations of ocean water induced by the seasonal fluctuations in the air temperature above the water surface. These changes in water temperature can be traced to depths of 250–300 m. The convection is the essential factor determining the depth of the seasonal thermocline. In numerical calculations the greatest turbulence is encountered for convection in the polar regions, where the ocean surface is subject to continuous chilling, and where the sinking convection penetrates to the deep ocean layers, even to the sea floor, generating, as we have explained, the global meridional lateral convection in the ocean.

For the atmosphere, however, a full analog to this

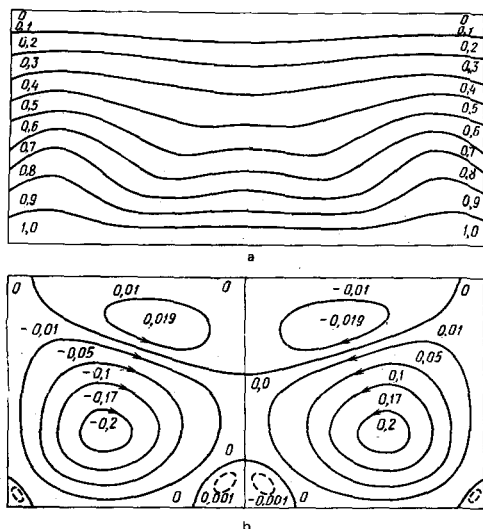


FIG. 12. The temperature and stream-function fields calculated for convection in water close to the density-inversion temperature.  $Cr = 4000$ ,  $Pr = 11.59$ .

oceanic process is not the convection involved in the growth of thunderclouds, penetrating to heights of 7–8 km, but the convection that induces the meridional air circulation, or the convection which develops in regions of constant surface heating and cooling, with formation of quasisteady centers of atmospheric pressure (such as the Iceland minimum and the East Siberian maximum) that gradually encompass a substantial body of the atmosphere (5–6 km thick) and result in horizontal air motions of considerable extent.

Numerical simulations using mathematical models of such convection [Eqs. (1)] have shown that initially, through cooling from above or warming from below, heat will be exchanged in water or air by molecular heat conductivity, as suggested, in particular, by the parallel isotherm surfaces. If the critical Grashof number  $Gr$  is relatively small, cellular convection will develop,<sup>93,96</sup> as illustrated in Fig. 12. When  $Gr$  becomes large enough, the processes will no longer be steady, but self-oscillating. Figure 13a displays part of a time-lapse sequence, calculated by computer,<sup>97</sup> of the self-oscillation that will occur during convection of water in a rectangular chamber when  $Gr = 16,000$ . We see that the flow will be exceedingly tangled and complex. Nevertheless, the mean temperature fields and stream functions turn out to be regular (Fig. 13b). In a sense they form a continuation in time of the steady laminar flow pattern that developed for small  $Gr$  values (Fig. 12). While these calculations were performed for a box of limited volume warmed from below,<sup>97</sup> the convection process that comes into play here should be quite general in character.

At first glance it may seem appealing to work out motions by computer simulation for more and more values of the parameters as the restricted size of the region causes the convection to penetrate inward, and then to take the appropriate averages. But one can easily see that such an approach is unrealistic. In order to simulate the ocean-atmosphere system by means

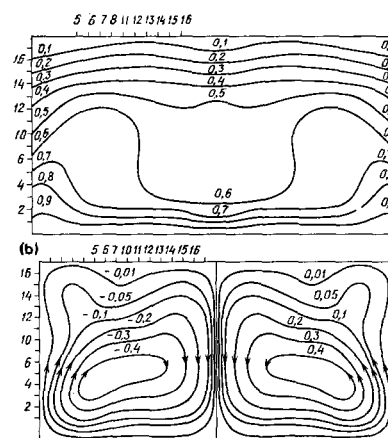
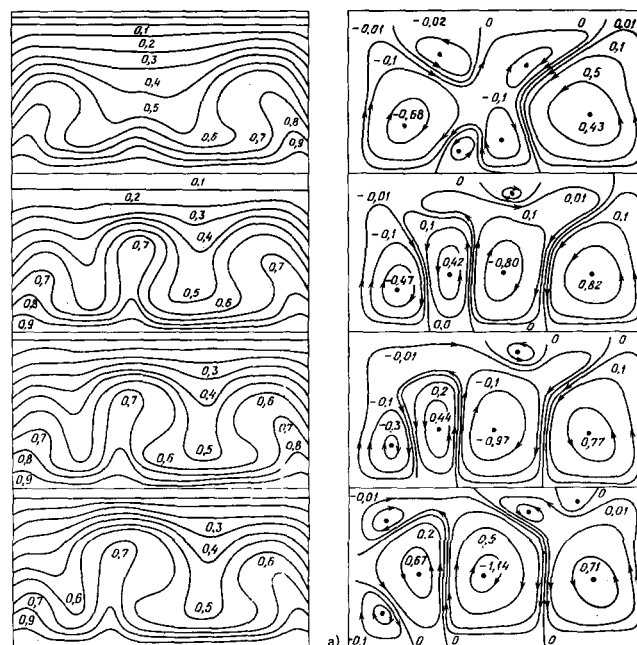


FIG. 13. a) Successive frames showing the temperature and stream-function fields  $T$ ,  $\psi$  calculated for convection in water close to the density-inversion temperature for  $Gr = 16\,000$ ; b) the corresponding fields  $T$ ,  $\psi$  averaged over the self-oscillation period.

of calculations with the molecular dynamical coefficients, one would need a computer memory of no less than  $10^{23}$  kilobytes. By comparison, the standard BESM-6 computer has a working memory of just 128 kilobytes. For the foreseeable future, then, the best one can do is to solve the averaged equations.

As we have pointed out, for large values of the characteristic dimensionless numbers the hydrodynamic processes can be grouped into a hierarchy with various times and linear scales. Thus, for the convective motion depicted in Fig. 13 the circulation is averaged over a single self-oscillation period, defined after the oscillations have become established.

Let us illustrate the averaging procedure with a sample calculation of the thermocline dynamics<sup>75</sup> for autumn cooling in the temperate zone. The water has a kinematic viscosity  $\nu \approx 10^{-4}$  m<sup>2</sup>/sec and the temperature

differential is  $\approx 10-20^\circ\text{C}$ , so  $Gr \approx 10^7 L^3$ , where  $L$  is measured in meters. Thus if  $L = 0.5$  km,  $Gr \approx 10^{15}$ .

For values  $Gr \approx 10^5-10^6$ , corresponding to scales  $L \approx 30$  cm, self-oscillations will be excited in the water. These oscillations can be modeled by computer. Upon averaging over the self-oscillation period one obtains a steady circulation for which certain mean Grashof and Prandtl numbers can be calculated<sup>75,98</sup>:

$$Gr = \frac{\frac{1}{T} \int_{t_1}^{t_1+T} dt \int_{\Omega_L} dx dy \left[ \Delta\varphi - \left( \frac{\partial\psi}{\partial y} \frac{\partial\varphi}{\partial x} - \frac{\partial\psi}{\partial x} \frac{\partial\varphi}{\partial y} \right) \right]}{\frac{1}{T} \int_{t_1}^{t_1+T} dt \int_{\Omega_L} dx dy \frac{\partial T}{\partial x} dx dy} \quad (16)$$

Accordingly, one can proceed as follows to calculate the effective turbulent exchange coefficient  $D$  for convection in the working layer of the ocean. The space to be investigated is divided into layers, whose dimensions are dictated by the computer capacity. Velocities and temperatures are averaged over the self-oscillation period in each layer. Then the viscosity and conductivity in the layer are determined, giving averaged equations. The turbulent viscosity and conductivity for the averaged equations will be about an order of magnitude greater than the molecular values. Next the original region is divided into subregions approximately five times as large as the initial ones, and the procedure is repeated. Four steps of the process are enough to provide the requisite oceanic temperature profile.

c. In current practice, global models typically use a  $4^\circ-5^\circ$  grid, and in the atmosphere from two (the Mintz-Arakawa model) to eleven (the Smagorinskii model) levels are considered. In the ocean, two levels are customary: a mixed upper layer and the deep waters. A great many very important processes governing the global circulation will then be gridded and call for parametric specification, including convection, which moreover cannot be handled in the quasistatic approximation ordinarily used in such models.

One other fundamental difficulty, discovered by Lorenz<sup>99</sup> in 1963, arises in efforts to implement such programs for arriving at hydrodynamic predictions. Lorenz investigated the convective motion in a two-dimensional model. If the convection takes place in a vertical  $(x, z)$  plane, where  $z$  is the vertical coordinate, then the equations of thermohydrodynamics will take the standard form

$$\begin{aligned} \frac{\partial}{\partial x} \nabla^2 \psi &= - \frac{\partial (\psi, \nabla^2 \psi)}{\partial (x, z)} + \nu \nabla^4 \psi + g\beta \frac{\partial \theta}{\partial x}, \\ \frac{\partial \theta}{\partial t} &= - \frac{\partial (\psi, \theta)}{\partial (x, z)} + \frac{\Delta T}{H} \frac{\partial \psi}{\partial x} + \kappa \nabla^2 \theta, \end{aligned} \quad (17)$$

where  $\psi$  is the plane-flow stream function,  $\theta$  denotes the deviation of the temperature  $T$  from equilibrium, and the constants  $g$ ,  $\beta$ ,  $\nu$ ,  $\kappa$  are respectively the acceleration of gravity, thermal expansion coefficient, kinematic viscosity, and thermal conductivity. If one seeks a solution by the Bubnov-Galerkin method, truncating the series so that they comprise three terms:

$$\begin{aligned} a(1+a^2)x^{-1}\psi &= x\sqrt{2} \sin(\pi a H^{-1}x) \sin(\pi H^{-1}z), \\ \pi R_c^{-1} Ra \Delta T^{-1} \theta &= Y \sqrt{2} \cos(\pi H^{-1}z) \sin(\pi H^{-1}z) - z \sin(2\pi H^{-1}z), \end{aligned} \quad (18)$$

then one obtains the system of ordinary differential

equations

$$\left. \begin{aligned} \dot{X} &= -\delta X + \delta Y, \\ \dot{Y} &= -XZ + rX - Y, \\ \dot{Z} &= XY - bz, \end{aligned} \right\} \quad (19)$$

where  $H$ ,  $aH$  represent the vertical and horizontal scales of the convection zone,  $b = 4/(1-a^2)$ ,  $\sigma = \nu/\kappa$  is the Prandtl number, and  $r = Ra/Ra_c$ ; the Rayleigh number is  $Ra = g\beta H^3 \Delta T/\nu\kappa$ , and its critical value is  $Ra_c = 27\pi^4/4$ . The equations are written in terms of the dimensionless time

$$\tau = \pi^2 H^{-2} (1+a^2) \kappa t.$$

Physically, the system (19) can be interpreted as describing the convection of a fluid in a thin tube, bent into a ring, placed in a vertical plane, and heated from below. If the temperature differential  $\Delta T$  between the lower and upper parts of the ring is adequate, then the lighter-weight fluid, warmed at the base of the ring, will rise, forcing the fluid cooling on top to sink. As a result the fluid will begin to revolve within its envelope in a direction depending on the initial disturbance. If the ring is heated below somewhat more strongly, the situation will become appreciably more complicated: the fluid will revolve in the opposite direction. This behavior can be explained as follows. When  $\Delta T$  is large, the fluid will tend to "unwind" so vigorously that it slips past the lower position without being heated there. As a result it is unable to overcome the viscosity and gravity forces and thereby to reach the top. Meanwhile the fluid at the base of the ring will continue to be heated and to float upward, but now in the opposite direction. Experiments show<sup>100</sup> that if  $\Delta T$  is large enough, these direction reversals will occur at random. Figure 14 plots the function  $Y$  calculated by Lorenz<sup>99</sup> for  $\sigma = 10$ ,  $b = 8/3$ ,  $r = 28$ . Notice that the oscillations become irregular.

It is pertinent here to recall an experiment that Byzova<sup>101</sup> published back in 1950. Byzova was seeking to demonstrate the possibility, and establish the cause, of the self-oscillations occurring in the lateral-convection regime, and thereby in many meteorological and oceanological processes. Her work was stimulated by V. V. Shuleikin, who was the first to broach this concept and who began the study of self-oscillations based on actual observations in nature.

In Byzova's experiment, a rectangular aquarium filled with water was warmed on one side and cooled on the other. For certain ratios between the water depth, the length of the aquarium, and the temperature difference

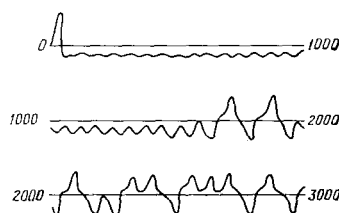


FIG. 14. A numerical solution of the convection equations showing the quantity  $Y$  as a function of time for the first 3000 units of dimensionless time.<sup>99</sup>

between the heater and coolant, self-oscillations were found to be excited in the developing lateral convection, with concomitant changes in the velocity and temperature of the circulating water. Byzova attributed this behavior to the alternating fast and slow motion of the fluid above the heater, and thereby to the alternation in the intensity with which thermal energy was fed to the fluid.

Chuprynin<sup>102</sup> has been doing experimental and theoretical research on self-oscillatory processes in the ocean-atmosphere system, and has developed a simplified one-dimensional mathematical model of the convection studied by Byzova. On analyzing the nonlinear one-dimensional equation of the model in the phase plane, Chuprynin found that self-oscillations could be excited in a vertical, closed path of fluid with changes not only in the amplitude of the velocity but also in its sign—rhythmic changes in the direction of motion of the fluid.

Evidently, then, all flows associated with convection in one way or another are not only very complicated, but unstable against external disturbances: solutions close together at the starting time will diverge rapidly. This may be an important fact, as Lorenz has pointed out, because it implies that long-term weather forecasting is prevented by the unavoidable inaccuracy and incompleteness of the measurements utilized as the initial conditions.

Lorenz's research has aroused interest in analyzing hydrodynamic models of the atmosphere from the same point of view. From numerous studies we now understand that in the course of the hydrodynamic calculations, initial errors will double<sup>103</sup> in 3–5 days. After 2–3 weeks of model time the rms error will exceed the climatological variability, and further calculation would be pointless.<sup>103</sup>

Among the natural structures found in the atmosphere, cyclones and anticyclones play an especially important role: they are powerful eddies which in themselves dominate the weather. Accordingly in attempting long-range forecasts it would be natural to try solving the averaged equations, as for example is the practice in calculating convection that penetrates to great heights or depths; but one would have to resolve the issue of the statistical underpinning for the averaged equations.

Over an interval of decades, a statistical ensemble of several thousand vortices will pass through the atmosphere. Hence the relative fluctuation in the number of cyclones or anticyclones as caused by random disturbances (and measured by  $N^{-1/2}$ , where  $N$  is the number of cyclones and anticyclones) will be a small quantity, and the mean kinematic parameters computed from a numerical model will depend only weakly on the initial data. Seasonal forecasts, on the other hand, will be sensitive to such fluctuations, because on the average there will be only a few cyclones each season over a limited territory (such as the European part of our country).

Thus in calculating trends in the weather extending over many years or the annual mean fluctuations of in-

dividual parameters, for which thousands of such eddies are available, forecasts will be justified; but for forecasts giving mean parameters for any particular year their number turns out to be sufficient in only a few cases and not in all parts of the globe.

## 5. CLOSING REMARKS

In our survey of the convective processes that take place on various scales in three of the earth's envelopes, we have seen that thermal and density-chemical inhomogeneities are the prime cause of many seemingly disparate phenomena on our planet. Yet all these processes obey the identical nonlinear differential equations. New results have lately been obtained that shed light on the fundamental character of the difficulties encountered in solving the thermohydrodynamic equations. An especially noteworthy finding is that the systems of nonlinear dynamical differential equations have a quasi-stochastic behavior. So far this discovery has brought more questions than answers. Even the very simple classical "strange attractor" of Lorenz contains much that is unclear. But the road toward progress in studies of convective processes has been marked out. It will surely entail analysis of the statistical properties of the solutions, and probably further application of asymptotic averaging techniques such as the Krylov-Bogolyubov method, which has been employed so brilliantly in statistical physics.

- <sup>1</sup>G. Z. Gershuni and E. M. Zhukhovitskiĭ, *The Convective Stability of an Incompressible Fluid* [in Russian], Nauka, Moscow (1972).
- <sup>2</sup>J. M. Hewitt, D. P. McKenzie, and N. O. Weiss, *J. Fluid Mech.* **68**, 721 (1975).
- <sup>3</sup>G. S. Golitsyn, *An Analysis of Convection, with Geophysical Applications and Analogies* [in Russian], Hydrol. Meteorol. Press, Leningrad (1980), p. 55.
- <sup>4</sup>Y. Ogura and N. A. Phillips, *J. Atmos. Sci.* **19**, 173 (1962).
- <sup>5</sup>A. Kh. Khrgian, *Physics of the Atmosphere* [in Russian], Hydrol. Meteorol. Press, Leningrad (1978).
- <sup>6</sup>E. Palmén and L. A. Vuorela, *Quart. J. Roy. Meteorol. Soc.* **89**, 131 (1963).
- <sup>7</sup>L. A. Vuorela and I. Tuominen, *Pure Appl. Geophys.* **57**, 167 (1964).
- <sup>8</sup>E. Palmén and C. W. Newton, *Atmospheric Circulation Systems: their Structure and Physical Interpretation* (Intl. Geophys. Ser. **18**), Academic Press (1969) [Russ. Transl., Hydrol. Meteorol. Press, Leningrad (1973)].
- <sup>9</sup>H. Riehl, *Jet Streams of the Atmosphere*, Govt. Printing Office, Washington (1961) [Dept. Atmos. Sci. Colorado State Univ. Tech. Rep. No. 32 (1962), p. 117].
- <sup>10</sup>V. P. Starr, *Physics of Negative Viscosity Phenomena*, McGraw-Hill (1968) [Russ. Transl., Mir, Moscow (1971)].
- <sup>11</sup>E. Yu. Zhdanova, *Abstracts of Candidate's dissertation* (1978).
- <sup>12</sup>V. V. Shuleĭkin, *Dokl. Akad. Nauk SSSR* **45**, 684 (1945).
- <sup>13</sup>V. V. Shuleĭkin, *Izv. Akad. Nauk SSSR, Ser. Geogr.-Geofiz.* (1937), No. 3, 277.
- <sup>14</sup>N. L. Byzova, *Dokl. Akad. Nauk SSSR* **58**, 393 (1947).
- <sup>15</sup>T. V. Bonchkovskaya, *Trudy Morsk. Gidrofiz. Inst. Akad. Nauk SSSR* **4**, 102 (1954).
- <sup>16</sup>A. A. Dmitriev, *ibid.*, **2**, 3 (1949).
- <sup>17</sup>Y. Nagata, *J. Marine Res.* **28**, 1 (1970).
- <sup>18</sup>R. V. Abramov, V. N. Bliznichenko, R. P. Bulatov, and L. N. Kazachkina, *Okeanologiya* **15**, 826 (1975) [Oceanology **15**, 554 (1976)].
- <sup>19</sup>K. N. Fedorov, *The Thermohaline Fine Structure of Ocean*

- Waters [in Russian], Nauka, Moscow (1976).
- <sup>20</sup>G. V. Neiman, Oceanic Currents [in Russian], Hydrol. Meteorol. Press, Leningrad (1973).
- <sup>21</sup>J. Bjerknes, *Tellus* **18**, 820 (1966).
- <sup>22</sup>H. Stommel, *Trans. Am. Geophys. Un.* **31**, 553 (1950).
- <sup>23</sup>J. C. Swallow and L. V. Worthington, *Deep-Sea Res.* **8**, 1 (1961).
- <sup>24</sup>V. A. Nekrasova and V. N. Stepanov, *Oceanic Research* [in Russian], No. 8, 34 (1963).
- <sup>25</sup>P. S. Linekin, *Dokl. Akad. Nauk SSSR* **101**, 461 (1955).
- <sup>26</sup>P. S. Linekin, *Dokl. Akad. Nauk SSSR* **117**, 971 (1957).
- <sup>27</sup>H. Stommel and G. Veronis, *Tellus* **9**, 401 (1957).
- <sup>28</sup>H. Stommel, A. Arons, and A. Feller, in: *Problems of Oceanic Circulation*, ed. W. B. Stockmann [Russ. Transl.], Mir, Moscow (1965).
- <sup>29</sup>J. Pedlosky, *J. Fluid Mech.* **35**, 185 (1969).
- <sup>30</sup>J. S. Allen, *J. Fluid Mech.* **56**, 429 (1972).
- <sup>31</sup>Y. J. F. Desaubies, *J. Fluid Mech.* **58**, 677 (1973).
- <sup>32</sup>D. Fultz, *J. Meteorol.* **9**, 379 (1952).
- <sup>33</sup>R. Hide, *Quart. J. Roy. Meteorol. Soc.* **79**, 161 (1953).
- <sup>34</sup>T. V. Bonchkovskaya, in: *Simulation of Phenomena in the Atmosphere and Hydrosphere* [in Russian], USSR Acad. Sci. Press (1962), p. 7.
- <sup>35</sup>V. P. Starr and R. R. Long, *Geophys. Res. Pap. (Air Force Cambridge Res. Cen.)* No. 24, 103 (1953).
- <sup>36</sup>F. V. Dolzhanskiĭ, V. N. Klyatskin, A. M. Obukhov, and M. A. Chusov, *Nonlinear Hydrodynamic-Type Systems* [in Russian], Nauka, Moscow (1975).
- <sup>37</sup>R. Hide and P. J. Mason, *Adv. Phys.* **24**, 47 (1975).
- <sup>38</sup>F. V. Dolzhanskiĭ and G. S. Golitsyn, *Izv. Akad. Nauk SSSR Fiz. Atmos. Okeana* **13**, 795 (1977) [*Izv. Acad. Sci. USSR Atmos. Oceanic Phys.* **13**, 550 (1978)].
- <sup>39</sup>H.-L. Kuo, *J. Marine Res.* **14**, 14 (1955).
- <sup>40</sup>H.-L. Kuo, *J. Meteorol.* **13**, 521 (1956).
- <sup>41</sup>E. N. Lorenz, *J. Atmos. Sci.* **19**, 39 (1962).
- <sup>42</sup>A. M. Gusev, in: *Proc. [Trudy] USSR Hydrol. Meteorol. Service, Sea Hydrol. Ser. No. 1*, 148 (1946).
- <sup>43</sup>J. W. Strutt (Lord Rayleigh), *Phil. Mag.* (6) **32**, 529 (1916).
- <sup>44</sup>V. V. Alekseev and V. M. Blinkov, *Vestn. Mosk. Gos. Univ., Ser. Fiz. Astron.* (1972), No. 6, 644 [Moscow Univ. Phys. Bull. **27**, No. 6, 13 (1972)].
- <sup>45</sup>C. Quon, *Phys. Fluids* **15**, 12 (1972).
- <sup>46</sup>P. S. Linekin, *Izv. Akad. Nauk SSSR, Ser. Geogr.-Geofiz.* **11**, 103 (1947).
- <sup>47</sup>J. W. Elder, *J. Fluid Mech.* **23**, 77, 99 (1965).
- <sup>48</sup>E. R. G. Eckart and W. O. Carlson, *Intl. J. Heat Mass Transf.* **2**, 106 (1961).
- <sup>49</sup>G. Z. Gershuni, E. M. Zhukhovitskiĭ, and E. L. Tarunin, *Izv. Akad. Nauk SSSR Mekhan. Zhidk. Gaza* (1968), No. 5, 130 [*Fluid Dyn.* **3**, No. 5, 86 (1972)].
- <sup>50</sup>G. de V. Davis, *Intl. J. Heat Mass Transf.* **11**, 1675 (1968).
- <sup>51</sup>M. E. Newell and F. W. Schmidt, *Trans. Am. Soc. Mech. Engrs. C* **92**, 159 (1970).
- <sup>52</sup>G. F. Carrier, *Boundary-Layer Problems in Applied Mechanics* [Russ. Transl., IL, Moscow (1955)].
- <sup>53</sup>A. E. Gill, *J. Fluid Mech.* **26**, 515 (1966).
- <sup>54</sup>M. Dixon and S. D. Proberg, *Intl. J. Heat Mass Transf.* **18**, 709 (1975).
- <sup>55</sup>D. E. Cormack, L. G. Leal, and J. Imberger, *J. Fluid Mech.* **65**, 209 (1974).
- <sup>56</sup>D. E. Cormack, L. G. Leal, and J. H. Steinfeld, *J. Fluid Mech.* **65**, 231 (1974).
- <sup>57</sup>J. Imberger, *J. Fluid Mech.* **65**, 247 (1974).
- <sup>58</sup>A. M. Gusev and V. M. Blinkov, "Topics in the motion of fluids nonuniformly heated horizontally" [in Russian], All-Un. Inst. Sci. Tech. Inform. [VINITI] MS Depository No. 9-306 (1978).
- <sup>59</sup>V. M. Blinkov and A. M. Gusev, *Izv. Akad. Nauk SSSR Fiz. Atmos. Okeana* **15**, 307 (1979) [*Izv. Acad. Sci. USSR Atmos. Oceanic Phys.* **15**, 210 (1980)].
- <sup>60</sup>V. M. Blinkov, Abstract of Candidate's dissertation (1980).
- <sup>61</sup>S. Chandrasekhar, *Hydrodynamic and Hydromagnetic Stability*, Oxford Univ. Press (1961).
- <sup>62</sup>O. G. Sorokhtin, *Izv. Akad. Nauk SSSR Fiz. Zemli* (1974), No. 5, 29 [*Izv. Acad. Sci. USSR Phys. Solid Earth* **10**, 297 (1975)].
- <sup>63</sup>V. P. Keondzhyan and A. S. Monin, *Dokl. Akad. Nauk SSSR* **220**, 825 (1975) [*Dokl. Earth Sci.* **221**, 1 (1976)].
- <sup>64</sup>V. P. Keondzhyan and A. S. Monin, *Izv. Akad. Nauk SSSR Fiz. Zemli* (1976), No. 4, 3 [*Izv. Acad. Sci. USSR Phys. Solid Earth* **12**, 229 (1977)].
- <sup>65</sup>G. S. Golitsyn, *Dokl. Akad. Nauk SSSR* **234**, 552 (1977) [*Dokl. Earth Sci.* **234**, 7 (1979)].
- <sup>66</sup>S. A. Ushakov and Yu. I. Galushkin, in: *Adv. Sci. Tech. [Itogi Nauki i Tekhniki], Earth Physics Ser. 3, The Lithosphere from Geophysical Data, Part 1, Plate Kinematics and the Oceanic Lithosphere* [in Russian], VINITI, Moscow, (1978).
- <sup>67</sup>S. A. Ushakov and Yu. I. Galushkin, *ibid.*, Part 2, The Continental Lithosphere [in Russian], VINITI (1979).
- <sup>68</sup>D. Fultz, R. R. Long, G. V. Owens, *et al.*, *Meteorol. M. Monogr. Am. Meteorol. Soc.* **4**, No. 21 (1959) (p. 36).
- <sup>69</sup>M. E. Stern, *Tellus* **11**, 175 (1959).
- <sup>70</sup>B. Guinot and M. Feissel, *J. Obsvrs.* **51**, 13 (1968) [Publ. Obs. Haute Provence **9**, No. 36 (1968)].
- <sup>71</sup>G. Schubert and J. A. Whitehead, *Science* **163**, 71 (1969).
- <sup>72</sup>G. Schubert, *J. Atmos. Sci.* **26**, 767 (1969).
- <sup>73</sup>E. J. Hinch and G. Schubert, *J. Fluid Mech.* **47**, 291 (1971).
- <sup>74</sup>F. H. Busse, *J. Atmos. Sci.* **29**, 1423 (1972).
- <sup>75</sup>V. V. Alekseev, N. S. Blokhina, A. M. Gusev, and E. Yu. Zhdanova, *Free Convection in the Atmosphere and Ocean* [in Russian], Moscow Univ. Press (1979), p. 139.
- <sup>76</sup>P. Gierasch and C. Sagan, *Icarus* **14**, 312 (1971).
- <sup>77</sup>L. J. Martin, *Icarus* **22**, 175 (1974).
- <sup>78</sup>D. Fultz, "Experimental combining of convection and rotation and some possible implications," in: *Proc. Midwest Conf. Dynamics* (1951), **1**, 235.
- <sup>79</sup>R. Hide, *Fluid Models in Geophysics*, Johns Hopkins Univ. Press (1953).
- <sup>80</sup>T. V. Bonchkovskaya, *op. cit.*,<sup>34</sup> p. 32.
- <sup>81</sup>T. V. Bonchkovskaya, in: *Studies of Heat Exchange in the Atmosphere* [in Russian], Nauka, Moscow (1964), p. 29.
- <sup>82</sup>T. G. Akimova, V. V. Alekseev, and A. M. Gusev, *Izv. Akad. Nauk SSSR Fiz. Atmos. Okeana* **11**, 787 (1975) [*Izv. Acad. Sci. USSR Atmos. Oceanic Phys.* **11**, 496 (1976)].
- <sup>83</sup>A. M. Gusev, *op. cit.*,<sup>42</sup> p. 96.
- <sup>84</sup>A. M. Gusev, *op. cit.*,<sup>34</sup> p. 49.
- <sup>85</sup>A. M. Gusev, in: *Ten Years of Progress in Antarctic Research (Proc. All-Un. Conf.)* [in Russian], Nauka, Moscow (1967).
- <sup>86</sup>M. Wada, *J. Meteorol. Soc. Japan* **57**, 505 (1979).
- <sup>87</sup>R. W. Jones, *J. Atmos. Sci.* **37**, 930 (1980).
- <sup>88</sup>S. L. Lebedev, *Izv. Akad. Nauk SSSR Fiz. Atmos. Okeana* **2**, 14 (1966) [*Izv. Acad. Sci. USSR Atmos. Oceanic Phys.* **2**, 8 (1966)].
- <sup>89</sup>N. V. Vel'tishchev and G. V. Ugryumova, *Meteorologiya Gidrologiya* (1970), No. 9, 10 [*Meteorology Hydrology* (1970)].
- <sup>90</sup>E. P. Anisimova, N. S. Blokhina, A. M. Gusev, *et al.*, *Vestn. Mosk. Univ., Ser. Fiz. Astron.* **35**, No. 5, 68 (1980) [Moscow Univ. Phys. Bull. **35**, No. 5, 64 (1981)].
- <sup>91</sup>G. G. Khundzhua, E. G. Andreev, and A. A. Budnikov, *Okeanologiya* **19**, 164 (1979) [*Oceanology* **19**, 101 (1980)].
- <sup>92</sup>G. G. Khundzhua and E. G. Andreev, *Dokl. Akad. Nauk SSSR* **255**, 829 (1980) [*Dokl. Earth Sci.* **255**, 28 (1982)].
- <sup>93</sup>A. M. Gusev and N. S. Blokhina, in: *Proc. Intl. Sympos. Diffusion of Mixtures in the Sea (Inform. Bull. No. 5)* [in Russian], Inst. Oceanography USSR Acad. Sci. (1977).
- <sup>94</sup>"The ETEKOS experimental ecosystem," in: *Man and the Biosphere* [in Russian], No. 4, Moscow Univ. Press (1980).
- <sup>95</sup>K. N. Fedorov, "The fine structure of geophysical fields in the ocean," in: *Oceanology—Oceanic Physics* [in Russian],

Vol. 1, Nauka, Moscow (1978).

- <sup>96</sup>A. S. Blokhin and N. S. Blokhina, *Dokl. Akad. Nauk SSSR* **193**, 805 (1970) [*Dokl. Earth Sci.* **193**, 11 (1971)].
- <sup>97</sup>A. S. Blokhin *et al.*, *Dokl. Akad. Nauk SSSR* **210**, 75 (1973) [*Dokl. Earth Sci.* **210**, 1 (1974)].
- <sup>98</sup>V. V. Alekseev, N. S. Blokhina, A. M. Gusev, and E. Yu. Zhdanova, in: *Oceanic Research Programs* (in Russian), Moscow Univ. Press (1980), p. 161.
- <sup>99</sup>E. N. Lorenz, *J. Atmos. Sci.* **20**, 130 (1963).
- <sup>100</sup>H. F. Creveling, J. F. de Paz, J. Y. Baladi, and R. J. Schoenhals, *J. Fluid Mech.* **67**, 65 (1975).
- <sup>101</sup>N. L. Byzova, *Dokl. Akad. Nauk SSSR* **72**, 675 (1950).
- <sup>102</sup>V. I. Chuprynin, *Abstract of Candidate's dissertation* (1972).
- <sup>103</sup>L. Bengtsson, *Tellus* **33**, 19 (1981).

Translated by R. B. Rodman